Directivity Pattern Simulation of the Ears with Two Pairs' Hearing Aid Microphone Arrays by BEM

Soon Suck Jarng*, You Jung Kwon*

*Dept. of Information, Control & Instrumentation, Chosun University, South Korea

Abstract

The noise reduction of the In-The-Ear (ITE) hearing aid (HA) can be achieved by arrays of microphones. Each of the right and the left ears was assumed to have two HA microphones. These arrays of HA microphones produce particular patterns of directivity by some time delay between two microphones. The directivity pattern geometrically increase the S/N ratio. The boundary element method (BEM) was used for the three dimensional simulation of the HA directivity pattern with the two pairs' microphone arrays. The separation between two microphones was fixed to 10 mm. The time delay between the two microphones was calculated to produce the most narrow directivity pattern in the fore front of the head. The variation of the time delay was examined in accordance with input frequencies. This numerical analysis may be then applied for the calculation of the time delay parameter of the digital hearing aid DSP chip.

I. Introduction

One of the advanced features of the digital hearing aid (HA) chip is its parameter—adjusting function. The user can change the parameter values of the digital HA chip for a better performance of some particular HA functioning. The main function of the HA is the amplification of the electrical signal. There are also many other specifications, but one particular feature we consider in this paper is the time delaying between two input channels. The outputs of two microphones can be input into a HA DSP chip such as Gennum GB3211[1]. Two microphones were used for making directional HAs[2]. The directional HA may have the increased sensitivity to the sound coming from a particular direction. This geometrical feature effectively improves the noise reduction in the presence of environmental noise. Each of the right and the left ears may have an ITE HA with two microphones. These two twin microphones' arrays simultaneously activate the formation of the directivity pattern. The directivity pattern of the digital HA can be changed depending on how those four microphones are located. It is common that each pair of two microphones has a short space of separation. Both the right and the left ears would have the same type of digital HAs. But there is a comparatively long space of the head between two ears.

Then a question arises. How much shall we have the short space between two microphones once we know the size of the head in order to produce the most sensitive directivity pattern or how much is the time delay between two microphones if we fix the space distance? We applied the boundary element method (BEM) for the solution of the question. The numerical method was very briefly mentioned and the application of the present problem was followed.

Corresponding author: Soon Suck Jarng (ssjarng@chosun.ac.kr)
Dept. of Information Control & Instrumentation, Chosun University.,
375 SeoSeok-Dong, Dong-Ku, Gwang-Ju

II. Boundary Element Method (BEM)

The sound pressure is scattered when incident sound pressure hits on an object such as the head. Then the sound field around the head is mixed with both the incident and the scattered sound pressure. The goal of the numerical method is to calculate the mixed sound pressure around the head. The size and the shape of the head and the ear as well as the input frequency may affect the sound pressure field.

The boundary element solution of the sound pressure field is based on the Helmholtz partial differential equation[3]. For sinusoidal steady-state problems, the Helmholtz equation, $\nabla^2\Psi + k^2\Psi = 0$ represents the wave mechanics. Ψ is the spatial pressure field that does not include time variation, $e^{j\omega t}$. In order to solve the Helmholtz equation in an infinite air media, a solution to the equation must satisfy not only the structural surface boundary condition (BC), $\partial\Psi/\partial n = \rho_f \omega^2 a_n$ but also the radiation condition at infinity, $\lim\limits_{|\vec{r}|\to\infty} \int_S (\partial\Psi/\partial r + jk\Psi)^2 dS = 0$. $\partial/\partial n$ represents differentiation along the outward normal to the boundary. a_n is normal displacement.

The Helmholtz integral equation derived from the Green's second theorem provides such a solution for radiating pressure waves:

$$\int_S \left(\Psi(q)\frac{\partial G_k(p,q)}{\partial n_q} - G_k(p,q)\frac{\partial\Psi(q)}{\partial n_q} \right) dS_q = \beta(p)\,\Psi(p)$$

(1)

where $G_k(p,q) = e^{-jkr}/4\pi r$, $r=|p-q|$

p is any point in either the interior or the exterior and q is the surface point of integration. β (p) is the exterior solid angle at p. k is the wave number.

The discrete BEM formulation of the Helmholtz surface integral equation can be represented as

$$\{\Psi\} = +\rho_f\omega^2[A]^{-1}[B]\{a\} - [A]^{-1}\{\Psi_{inc}\}$$

(2)

where ρ_f is the air density and Ψ_{inc} is the incident sound pressure. [A] and [B] are acoustic impedance matrices[4].

Each three dimensional boundary surface element is composed of 8 quadratic nodes and each node has nodal surface pressure (Ψ) variable. If we assume a rigid surface boundary condition, equation (2) becomes

$$\{\Psi\} = -[A]^{-1}\{\Psi_{inc}\}$$

(3)

Once $\{\Psi\}$ is known, the acoustic pressure in the near or far field is determined by $\beta(p)=1$ of equation (1) for given values of surface nodal pressure and zero surface nodal displacement;

$$\Psi(p_i) = \sum_{m=1}^{nt}\sum_{j=1}^{8} A^j_{m,j}\Psi_{m,j}$$

(4)

where nt is the total number of the boundary elements.

III. Boundary Element Mesh Generation

Two particular head-like structures were considered; sphere, head CAD model. All three structures were meshed for boundary surface element grids. The head model element mesh was formed by a CAD program[5].

Figure 1 shows the surface element meshes of a sphere. The diameter of the sphere is 18cm. Figure 1(b) shows the magnified view of two microphones indicated by an arrow of Fig. 1(a). Figure 1(c) shows twin microphones in the left ear and the right ear. For convenience the spherical model over-simplifies the head and the ear structures. The y axis indicator of Fig. 1(c) directs toward the fore front of the head and the other side is assumed to be the backward of the head. The angle of the directivity pattern starts from the front in anti-clockwise direction.

Figure 2 shows the head model. This model is meshed for surface boundary elements. Figure 2 shows the head model generated by a CAD program. The head model has the outer ear and the ear carnal, and the diameter of the head model from the front to the back is 18cm.

The BEM program was coded in Fortran in double precision and was executed by a PC with 2G RAM. The air density is 1.34
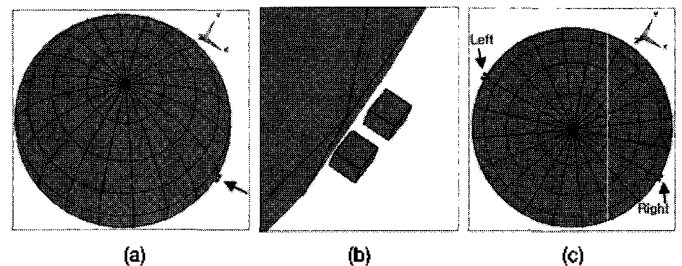

| (a) | (b) | (c) |

Fig. 1. (a) The surface element mesh of a sphere (Diameter = 18cm). (b) The magnified view of two microphones indicated by an arrow of (a). (c) Twin microphones in the left ear and the right ear.
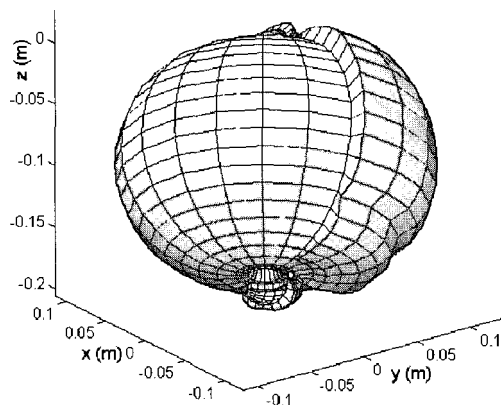
Fig. 2. Head model (Diameter = 18cm). This model generated by a CAD program.

$[Kg/m^3]$ and the sound speed in the air is 344 [m/sec]. Input frequencies are 500, 1000, 1500, 2000, 2500, 3000, 3500, and 4000 Hz.

IV. Results

Figure 3 shows the near filed of the sound pressure for the spherical model at 1 kHz. The upper side is the front and the lower side is the rear in two dimensions. The incident sound pressure is coming from the front.

Figure 4 shows directivity patterns of two front and rear microphones only without the spherical model. The distance between two microphones are 10mm respectively. The input frequency, f, is 4kHz. The rear microphone is set to be a reference microphone, so as to have zero time delay. The time delays, $2\pi f \Delta t$, between the front and the rear microphones are (a) 0, (b) 0.7π, (c) 0.8π, (d) 0.9π, (e) 1.1π, (f) 1.2π, (g) 1.3π, (h)
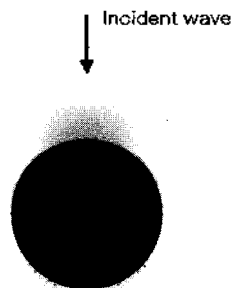

Fig. 3. The near filed of the sound pressure for the spherical model at 1 kHz in two dimensional view.

1.4π in radian. The amplitude and the phase of the front microphone is A_f and θ_f while those of the rear microphone is A_r and θ_r. The strength of the summed sound pressure from the
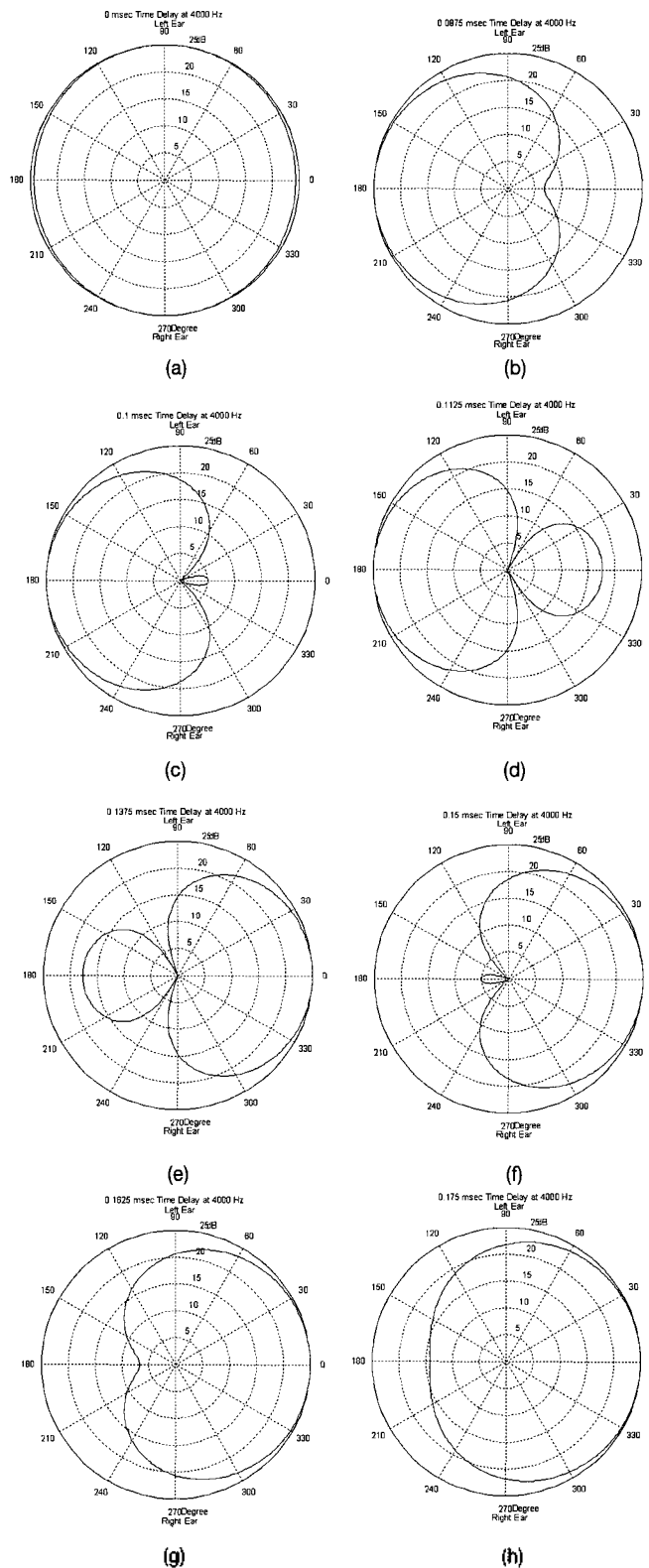

(a)

(b)

(c)

(d)

(e)

(f)

(g)

(h)

Fig. 4. Directivity patterns without the spherical model. Time delays [rad]= (a) 0, (b) 0.7π, (c) 0.8π, (d) 0.9π, (e) 1.1π, (f) 1.2π, (g) 1.3π, (h) 1.4π.

front and the rear microphones is calculated as:

$$\left| A_r \cos\left(2\pi f \cdot (t-0) + \theta_r\right) + A_f \cos\left(2\pi f \cdot (t-\Delta t) + \theta_f\right) \right| \tag{5}$$

The front microphone is delayed in time because it leads the phase. Figure 4 shows that the directivity pattern of the two microphones' array looks like symmetric omnidirectional shape in zero time delay. As the time delay increases, the directivity pattern changes in its shape but returns back to its initial shape due to periodicity. The commercial digital HA considers the directivity pattern effect of the two microphones only for each ear. It does not consider the effects of the size and the shape of the head and the ears.

Figure 5 shows directivity patterns of two twin microphones with the spherical model effect. The distance between two microphones is 10mm. The input frequency, f, is 4kHz. The time delays between the front and the rear microphones are (a) 0, (b) 0.32π, (c) 0.3704π, (d) 0.48π, (e) 0.88π, (f) 0.9104π, (g) 0.92 π, (h) 0.9304π, (i) 0.96π, (j) π, (k) 1.08π, (l) 1.16π, (m) 1.36π, (n) 1.6π, (o) 1.76π in radian. Because of the geometrical effect of the spherical model, the directivity patterns of the two twin microphones with the spherical model show different shapes in comparison with the two microphones without the spherical model. The strength of the summed sound pressure from the two twin microphones is calculated as:

$$\left| A'_r \cos\left(2\pi f \cdot (t-0) + \theta'_r\right) + A'_r \cos\left(2\pi f \cdot (t-\Delta t) + \theta'_r\right) \right| \times$$
$$\left| A'_r \cos\left(2\pi f \cdot (t-0) + \theta'_r\right) + A'_r \cos\left(2\pi f \cdot (t-\Delta t) + \theta'_r\right) \right| \tag{6}$$

where A'_r and θ'_r are the amplitude and the phase of the right–front microphones, A'_r and θ'_r are those of the right–rear microphones, A'_r and θ'_r are those of the left–front microphones and A'_r and θ'_r are those of the left–rear microphones.
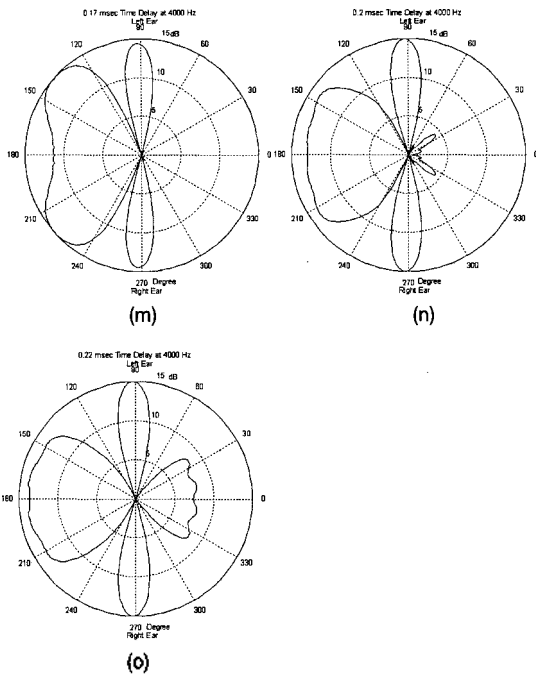
(m)

(n)

(o)

Fig. 5. Directivity patterns with spherical model. Time delays
[rad]= (a) 0, (b) 0.32π, (c) 0.3704π, (d) 0.48π, (e)
0.88π, (f) 0.9104π, (g) 0.92π, (h) 0.9304π, (i) 0.96π, (j)
π, (k) 1.08π, (l) 1.16π, (m) 1.36π, (n) 1.6π, (o) 1.76π.

(a)
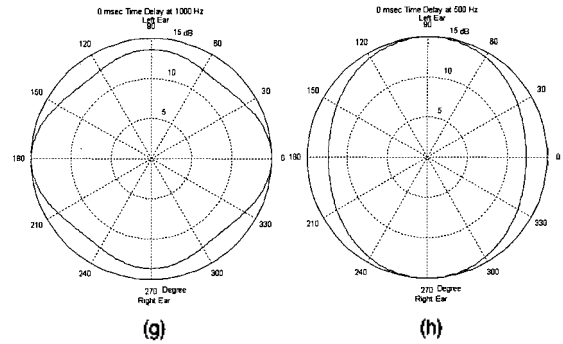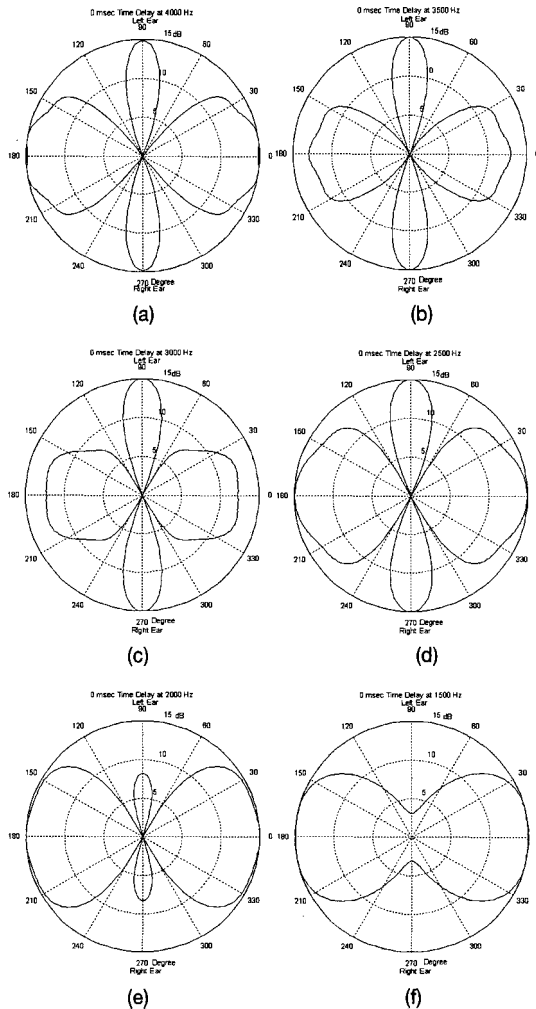
(b)

(c)

(d)

(e)

(f)

(g)

(h)

Fig. 6. Directivity patterns of the spherical model. Input
frequencies= (a) 4000 Hz , (b) 3500 Hz , (c) 3000 Hz
. (d) 2500 Hz , (e) 2000 Hz, (f) 1500 Hz , (g) 1000
Hz , (h) 500 Hz.

Figure 6 shows directivity patterns of the spherical model.
The time delay between the front and the rear microphones is
fixed to be zero but the input frequency is changed from 4kHz
down to 0.5kHz. As the input frequency decreases the
directivity pattern becomes omnidirectional because of the
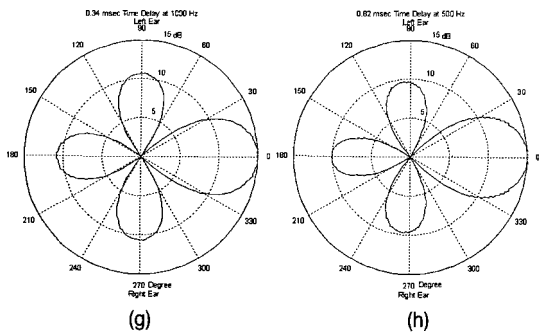increased wave length.

(a)

(b)

(c)

(d)

(e)

(f)

(g)   (h)
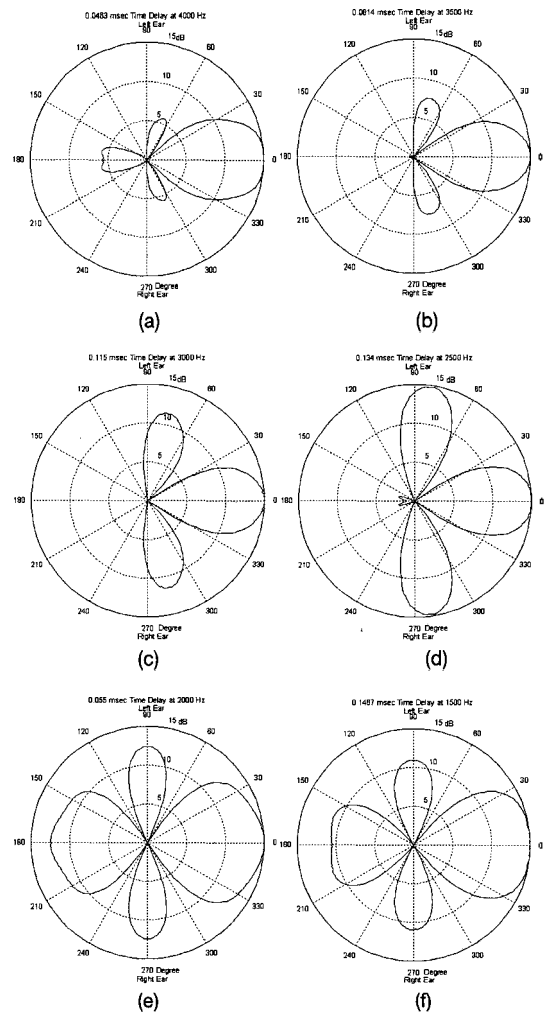
Fig. 7. Directivity patterns of the spherical model. Time delays [rad] & Frequencies [Hz]= (a) 0.37 π & 4000, (b) 0.57 π & 3500, (c) 0.69 π & 3000, (d) 0.67 π & 2500, (e) 0.22 π & 2000, (f) 0.44 π & 1500, (g) 0.68 π & 1000, (h) 0.82 π & 500.

Figure 7 shows directivity patterns of the spherical model. Optimal time delay is found to produce sharpest directivity pattern in accordance with each input frequency. Figure 7 indicates that the time delay of the digital HA needs to be varied as a function of the frequency if the user wants to have sharp directivity patterns in wide bandwidth. This suggests that a precisely controlled phase delay circuit should be included inside the digital HA for better directivity performance.
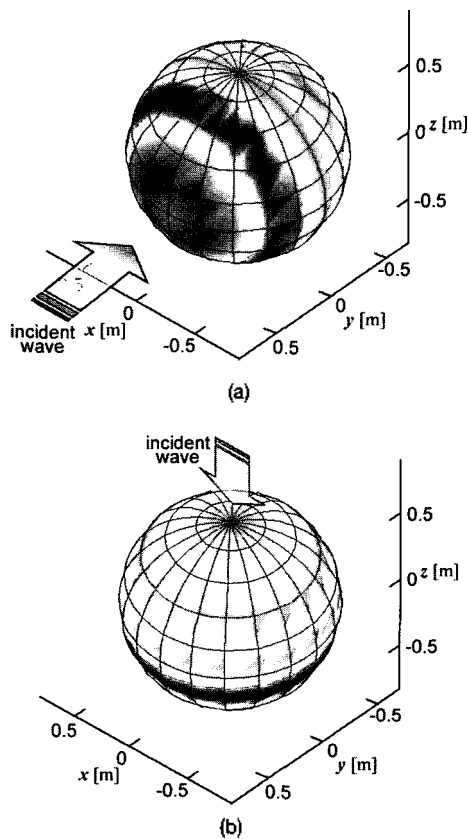
Figure 8 shows the surface sound pressure distribution of the spherical model at the oncoming incident sound pressure. Figure 8(a) has 0°Incident sound pressure while Figure 8(b) has 90° incident sound pressure directions.

Figure 9 shows the surface sound pressure distribution of the head model at the 0° oncoming incident sound pressure. Figure 10 shows directivity patterns of the head model in polar and in rectangular form. Figure 10 (a) is for zero time delay, and (b) is for 1.16 π [rad] time delay. The input frequency is 4 kHz. The time delay of 1.16 π [rad] is equivalent to 58% in 4kHz periodic phase. The particular time delay is chosen to produce the most sharp directivity pattern.

Figure 11 shows summed sound pressure of the spherical model (Δ) and the head model (□) as a function of frequency. Time delay is fixed at 0 [rad]. The resonance happened in the head model at 3kHz because the length of ear carnal from the outer ear to the tympanic membrane.

Table 1-(a) shows relative summed sound pressures of the spherical model and the head model as a function of frequency. Time delays are optimally chosen to produce the most sharp directivity patterns for different frequencies (Table 1-(b) and (c)).
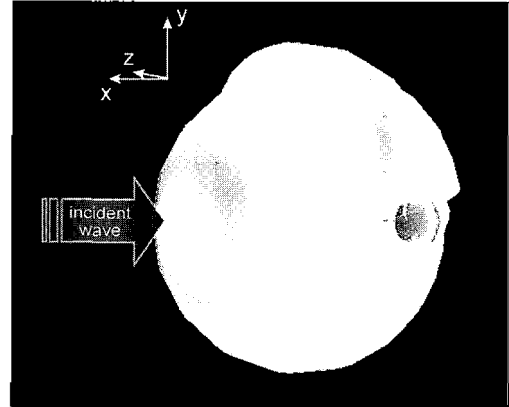

(a)

(b)

Fig. 8. The surface sound pressure distribution of the spherical model at the oncoming incident sound pressure. (a) 0°, (b) 90°incidence.

Fig. 9. The surface sound pressure distribution of the head model at the 0° oncoming incident sound pressure.
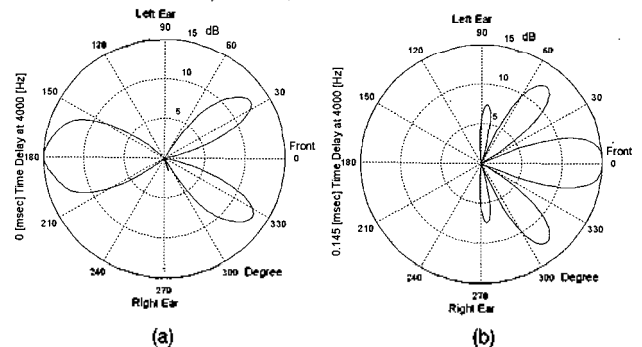

(a)   (b)

Fig. 10. Directivity patterns of the head model in polar. (a) for zero time delay, (b) for 1.16 π [rad] time delay. Input frequency = 4 kHz.
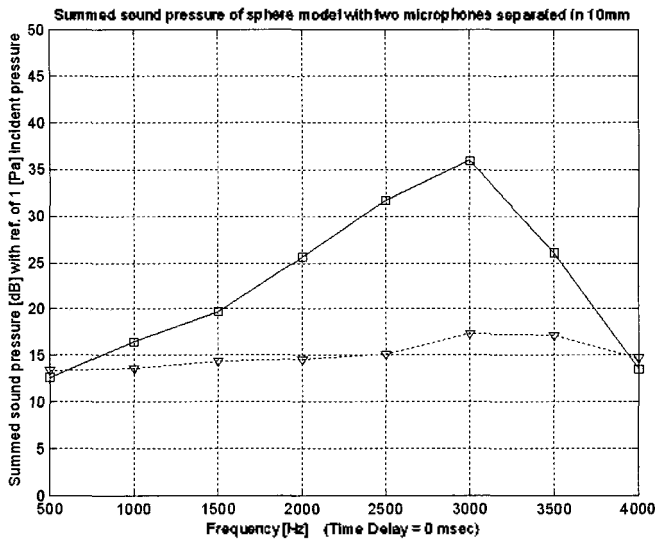
Fig. 11. Summed sound pressures of the spherical model (△) and the head model (□) as a function of frequency. The head model has the resonance effect of the ear carnal at 3kHz. Time delay = 0 [rad].

0 dB (ref. 1 Pa) is summed sound pressure with zero time delay. Relative summed sound pressures are below 0 dB because of phase cancellation. If the attenuation of the summed sound pressures with appropriate time delays are to be not much below 0 dB, then the degree of the directivity pattern sensitivity decreases. However the main purpose of the directive HA is to focus its geometrical sensitivity in the front. Therefore the attenuation is necessarily happened. Table 1—(b) shows time delays optimally chosen to produce the most sharp main lobe of the spherical model and the head model in time [msec]. Table 1—(c) shows time delays optimally chosen to produce the most sharp main lobe of the spherical model and the head model in periodic cycle [%]. The head model clearly shows the reduced attenuation at lower frequencies. It is because of the geometrical effect of the outer ear. Table 1—(d) shows −3dB main directivity lobe width with the optimally chosen time delays. The main beam lobe becomes smaller as the frequency increases.

Table 1—(e) shows the maximum attenuation of the first side beam lobe with the optimal time delays. Table 1—(f) shows directional angle of the first side lobe in reference with the main lobe at 0° with the optimal time delays. Relative summed sound pressures in the side lobe are also below 0 dB as the main lobe because of phase cancellation. The directional angle of the first

Table 1. Comparison of the spherical model and the head model.

Frequency[Hz]	(a) Relative summed sound pressure [dB]		(b) Time delays optimally chosen to produce the most sharp main lobe in time [msec]		(c) Time delays optimally chosen to produce the most sharp main lobe in periodic cycle [%]	
	Spherical model	Head model	Spherical model	Head model	Spherical model	Head model
500	13.48	12.67	-0.8200	-0.4400	-41.0	-22.0
1000	13.66	16.50	-0.3400	-0.1800	-34.0	-18.0
1500	14.39	19.73	-0.1467	-0.6430	-22.0	3.5
2000	14.58	25.60	-0.0550	-0.1475	-11.0	-29.5
2500	15.16	31.71	-0.1340	-0.0240	-33.5	-6.0
3000	17.37	35.93	-0.1150	-0.0247	-34.5	26.0
3500	17.15	26.06	-0.0814	-0.1710	-28.5	40.0
4000	14.70	13.57	-0.0463	-0.1450	-18.5	42.0

Frequency[Hz]	(d) -3dB main beam lobe width [degree]		(e) Attenuation of the maximum of the 1st side beam lobe [dB]		(f) Directional angle of the 1st side lobe in reference with the main lobe at 0 degree [degree]		(g) Attenuation of the maximum of the rear beam lobe [dB]	
	Spherical model	Head model	Spherical model	Head model	Spherical model	Head model	Spherical model	Head model
500	48.0	96.0	-44.20	-	95.0	-	-43.70	-11.70
1000	46.0	66.0	-22.10	-7.14	88.0	96.0	-21.90	-7.03
1500	70.0	102.0	-9.40	-2.29	92.0	98.0	-9.40	-2.80
2000	80.0	44.0	-2.50	-16.29	89.0	84.0	-2.40	-32.04
2500	42.0	59.0	-15.80	-8.92	80.0	74.0	-28.40	-13.90
3000	40.0	63.0	-21.90	-13.44	78.0	70.0	-35.70	-14.01
3500	40.0	41.0	-17.50	-16.18	73.0	63.0	-24.70	-27.25
4000	48.0	30.0	-10.40	-11.82	66.0	50.0	-10.20	-39.45

side lobe becomes close to the main lobe direction as the frequency increases. Table 1-(g) shows the maximum attenuation of the rear beam lobe with the optimal time delays. The maximum attenuation of the rear lobe is bigger than that of the side lobe as frequencies increase.

V. Conclusion

In Figure 7, the optimal time delay for the best directivity pattern needs to be found as a function of the frequency. The author suggests that a precisely controlled phase delay circuit should be included inside the digital HA for better directivity performance. The shape and the size of the head and the ear may affect the directivity performance of the digital HA because of wavelength. This means that the amplitude envelope of the HA amplification needs to include those geometrical effects of the head and the ear. It is physically difficult to vary the position of the twin microphones, but the time delay of the digital HA may be changed not only as a function of frequency but also as a function of the geometric parameter of the shape and the size of the head and ears. Then the BEM could be further applied as a parameter extraction tool for the precise control of the time delay in the digital HA. The BEM can be applied for the sound pressure field calculation for any arbitrary shape of the head and the ear.

Acknowledgment

References

1. Jarng S.S., "Gennum GB3211 ITE Hearing Aid Chip Interface and Electro-Acoustic Testing" , Proc. of Korean Sensor Society, 14, 59-62, 2003.
2. Frye G. J., "Testing Digital and Analog Hearing Instruments: Processing Time Delays and Phase Measurement" s, The Hearing Review, 8, 1-8, 2001.
3. Francis D.T.I., "A boundary element method for the analysis of the acoustic field in three dimensional fluid-structure interaction problems" , Proc. Inst. of Acoust., 12 (4), 76-84, 1990.
4. Francis D.T.I., "A gradient formulation of the Helmholtz integral equation for acoustic radiation and scattering" , J. Acoust. Soc. Am. 93 (4), Part 1, 1700-1709, 1993.
5. Jarng S.S., Yang H.J., Lee J.H. "Finite element mesh generation from 3D laser scanned data" , Journal of Korean CAD/CAM Society, 10 (1), 69-74, 2005.

[Profile]

●Soon Suck Jarng

1984.2 : Hanyang Uni. (S. Korea), Dept. of Electronics (B.Eng.)
1985.9 : Hull Uni. (U.K.), Dept. of Electronics (M.Eng.)
1988.9 : Birmingham Uni. (U.K.), Dept. of Physiology (M.Sc.)
1991.12 : Birmingham Uni. (U.K.), Dept. of Electronic Electrical Eng. (Ph.D.)
1992.3~Present Professor in the Dept. of Information Control & Instrumentation, Chosun University (South Korea)
※Main Research : Cochlear Bio-mechanics, Hearing Aids, Piezoelectric Sensor Device, Finite Element Method (FEM), Boundary Element Method (BEM)

●You Jung Kwon

1987.2: Yonsei Uni. (S. Korea), Dept. of Food & Science (B.Sc.)
2005.2: Chosun Uni. (S. Korea), Dept. of Information Control & Instrumentation (M.Eng.)
2005.3~Present: Ph.D. student in the Dept. of Information Control & Instrumentation, Chosun University (S. Korea)
※Main Research: Cochlear Bio-mechanics, Hearing Aids